Total aberrations compensation in digital holographic microscopy with a reference conjugated hologram

Tristan Colomb, Jonas Kühn, Florian Charrière and Christian Depeursinge

Ecole polytechnique fédérale de Lausanne,
Institute of imaging and applied optics,
CH-1015 Lausanne, Switzerland
tristan.colomb@a3.epfl.ch

http://apl.epfl.ch/page12232.html

Pierre Marquet

Centre de Neurosciences Psychiatriques, Département de psychiatrie DP-CHUV, Site de Cery,
1008 Prilly-Lausanne, Switzerland

Nicolas Aspert

Lyncée Tec SA,
PSE-A,
CH-1015 Lausanne, Switzerland

http://www.lynceetec.com

Abstract: In this paper we present a new method to achieve quantitative phase contrast imaging in Digital Holographic Microscopy (DHM) that allows to compensate for phase aberrations and image distortion by recording of a single reference hologram. We demonstrate that in particular cases in which the studied specimen does not have abrupt edges, the specimen's hologram itself can be used as reference hologram. We show that image distortion and phase aberrations introduced by a lens ball used as microscope objective are completely suppressed with our method. Finally the concept of self-conjugated reference hologram is applied on a biological sample (Trypanosoma Brucei) to maintain a spatial phase noise level under 3 degrees.

OCIS codes: (090.1760) Computer holography; (090.1000) Aberration compensation; (180.3170) Interference microscopy

References and links

1. E. Cuche, P. Marquet, and C. Depeursinge, "Spatial filtering for zero-order and twin-image elimination in digital off-axis holography," Appl. Opt. **39**, 4070–4075 (2000).
2. E. Cuche, P. Marquet, and C. Depeursinge, "Simultaneous amplitude-contrast and quantitative phase-contrast microscopy by numerical reconstruction of Fresnel off-axis holograms," Appl. Opt. **38**, 6994–7001 (1999).
3. G. Pedrini, S. Schedin, and H. J. Tiziani, "Aberration compensation in digital holographic reconstruction of microscopic objects," J. Mod. Opt. **48**, 1035–1041 (2001).

#69116 - $15.00 USD Received 21 March 2006; revised 3 May 2006; accepted 5 May 2006

4. P. Ferraro, S. D. Nicola, A. Finizio, G. Coppola, S. Grilli, C. Magro, and G. Pierattini, "Compensation of the inherent wave front curvature in digital holographic coherent microscopy for quantitative phase-contrast imaging," Appl. Opt. **42**, 1938–1946 (2003).
5. A. Stadelmaier and J. H. Massig, "Compensation of lens aberrations in digital holography," Opt. Lett. **25**, 1630–1632 (2000).
6. S. Grilli, P. Ferraro, S. D. Nicola, A. Finizio, G. Pierattini, and R. Meucci, "Whole optical wavefields reconstruction by digital holography," Opt. Express **9**, 294–302 (2001).
7. S. de Nicola, A. Finizio, G. Pierattini, P. Ferraro, and D. Alfieri, "Angular spectrum method with correction of anamorphism for numerical reconstruction of digital holograms on tilted planes," Opt. Express **13**, 9935–9940 (2005).
8. T. Colomb, E. Cuche, F. Charrière, J. Kühn, N. Aspert, F. Montfort, P. Marquet, and C. Depeursinge, "Automatic procedure for aberration compensation in digital holographic microscopy and applications to specimen shape compensation," Appl. Opt. **45**, 851–863 (2006).
9. T. Colomb, F. Montfort, J. Kühn, N. Aspert, E. Cuche, A. Marian, F. Charrière, S. Bourquin, and C. Depeursinge, "A numerical parametric lens for shifting, magnification and complete aberration compensation in digital holographic microscopy," J. Opt. Soc. Am. A (submitted) (2006).
10. J. Upatnieks, A. V. Lugt, and E. Leith, "Correction of lens aberrations by means of holograms," Appl. Opt. **5**, 589–593 (1966).
11. J. Ward, D. Auth, and F. P. Carlson, "Lens Aberration Correction by Holography," Appl. Opt. **10**, 896–900 (1971).
12. C. J. Mann, L. Yu, C.-M. Lo, and M. K. Kim, "High-resolution quantitative phase-contrast microscopy by digital holography," Opt. Express **13**, 8693 – 8698 (2005).

1. Introduction

Digital Holographic Microscopy (DHM) is a powerful technique for real-time quantitative phase contrast imaging, since a single intensity image, called hologram, allows the reconstruction of the phase shift induced by a specimen. Furthermore, the digital approach of holography permits through numerical processing of the hologram to filter out parasitic interferences, zero-order and twin image terms [1] or to compensate for curvature introduced by Microscope Objective (MO) [2, 3, 4], spherical aberration [5], astigmatism [6], anamorphism [7]. In recent papers, we presented the concept of numerical parametric lenses (NPL) placed in the reconstruction plane [8] and/or hologram plane [9] that allows with simple automatic procedures to correct shifting, magnification and full aberration. In this paper, we introduce the concept of Reference Conjugated Hologram (RCH), taking as a starting point the works of Ward and Upatnieks in Refs. [10, 11]. RCH allows a calibration of the DHM setup via phase aberrations and image distortion compensation without needing iterative procedures to adjust parameters. Furthermore we demonstrate, in the case of a setup presenting reduced aberrations, that the specimen's hologram itself can be defined as Self-Reference Conjugated Hologram (Self-RCH) for a specimen without abrupt edges.

2. Principle

Figure 1 presents typical DHM setups in transmission (a) or reflection (b) configurations. The architecture is based on a modified Mach-Zehnder interferometer. A MO collects the wave transmitted through or reflected by the specimen, produces an object wave $\boldsymbol{O}$ forming a magnified image of the specimen at a distance $d \cong 5$ cm behind the CCD camera. A lens or a similar MO [12] could be introduced in the reference arm (RL) allowing to obtain reference and object waves with similar curvatures in the CCD plane. To illustrate the aberrations correction method, we introduce a lens ball (Edmund lens ball SF8 of 2 mm diameter $n = 1.689$) as a non-corrected MO and a field lens between the beam splitter and the CCD in the transmission configuration [Fig. 1(a)] to produce strong aberrations (Fig. 2). A liquid index ($n = 1.6$) is used as immersion liquid. The sample is a USAF test target.

At the exit of the interferometer, the interference between the reference and object waves

#69116 - $15.00 USD Received 21 March 2006; revised 3 May 2006; accepted 5 May 2006

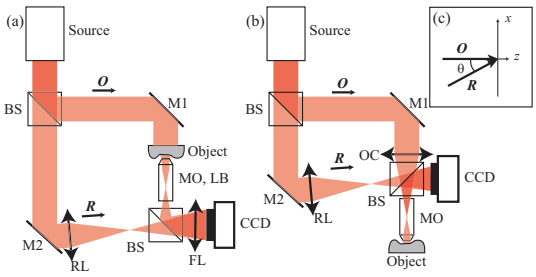

Fig. 1. Digital holographic microscope, (a) transmission and (b) reflection setups. ***O*** object wave; ***R*** reference wave; BS beam splitter; M1, M2 mirrors; MO microscope objective, RL lens in the reference wave, OC condenser in the object wave, FL field lens and LB lens ball.(c) Detail of the off-axis geometry.

produces a *NxN* pixels hologram digitalized by the CCD camera:

$$I_H(k,l) \quad = (\boldsymbol{R}+\boldsymbol{O})(\boldsymbol{R}+\boldsymbol{O})^* = |\boldsymbol{R}|^2 + |\boldsymbol{O}|^2 + \boldsymbol{R}^*\boldsymbol{O} + \boldsymbol{R}\boldsymbol{O}^*, \tag{1}$$

where *k*,*l* are integers defining the position of the hologram pixels. The two first terms form the zero-order term, the third and fourth terms are respectively the virtual and real image terms. Examples of holograms and their respective spectra (zero-order term is already filtered) are presented in Fig. 2

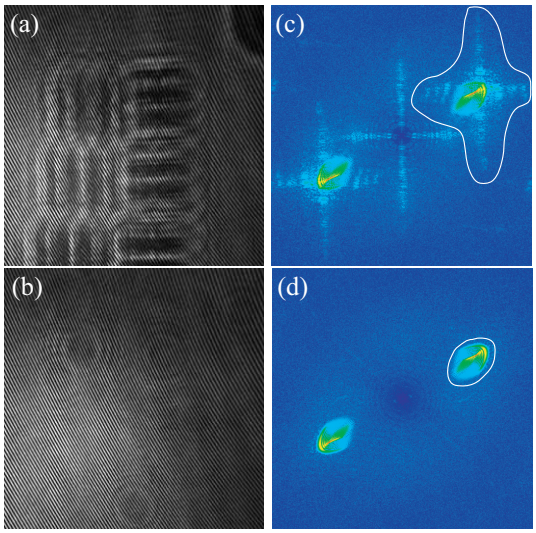

Fig. 2. 256x256 pixels area of 512x512 pixels holograms and spectra with lens ball as MO, the zero-order term is already filtered out; (a,b) are respectively the hologram with and without the USAF test target; (c,d) are the corresponding spectra. The white lines show the spectrum area of the virtual image that is retained after manual spatial filtering.

Usually, the reference and object wave are assumed to be plane or spherical waves. We assume here that the specimen introduces only a phase delay $\varphi(x,y)$ resulting from a height difference of the specimen in reflection configuration or from a refractive index or/and thickness difference in transmission configuration. Let us define here more generally perfect plane reference and object waves (the same reasoning can be applied to spherical waves) and a third

#69116 - $15.00 USD Received 21 March 2006; revised 3 May 2006; accepted 5 May 2006

wave $\boldsymbol{O}_0$, corresponding to the object wave without presence of specimen, by adding the phase aberrations terms $W_{\boldsymbol{R}}$ and $W_{\boldsymbol{O}_0}$ that are the phase difference between perfect plane (or spherical) waves and physical waves (corresponding for instance to defocus aberration, spherical aberration, astigmatism, and so on):

$$\boldsymbol{R}(x,y) = |\boldsymbol{R}| \cdot \exp\left[i(k_x x + k_y y)\right] \cdot \exp\left[iW_{\boldsymbol{R}}(x,y)\right], \quad (2)$$

$$\boldsymbol{O}_0(x,y) = |\boldsymbol{O}_0(x,y)| \cdot \exp\left[iW_{\boldsymbol{O}_0}(x,y)\right], \quad (3)$$

$$\boldsymbol{O}(x,y) = |\boldsymbol{O}(x,y)| \exp\left[i\varphi(x,y)\right] \cdot \exp\left[iW_{\boldsymbol{O}_0}(x,y)\right], \quad (4)$$

where k_x, k_y define the propagation direction associated to the angle θ defined in Fig. 1(c). In principle, phase aberrations are converted, at least partially, into amplitude aberrations during optical propagation, producing image distortion. Here, the small physical propagation of light between the MO and the CCD plane (few centimeters) and the assumption of small aberration coefficients allow to neglect the image distortion in the CCD plane. Therefore, we assume that there are only phase aberrations in the hologram plane.

The reconstructed wavefront Ψ of the virtual image is computed by multiplying the digital hologram by a digital reference wave $\boldsymbol{R}_D$ and by computing numerically the wave front at a distance d. This propagation can be achieved using the Single Fourier Transform Formulation (SFTF) or the Convolution Formulation (CF) (See Ref. [9] for details). To simplify the notation, the reconstructed wavefront is presented using CF without loosing generality:

$$\Psi_{\mathrm{CF}}(m,n) = A \cdot \mathrm{DFT}^{-1}\left\{\mathrm{DFT}\left[\boldsymbol{R}_D(k,l) I_H(k,l)\right] \cdot \exp\left[-i\pi\lambda d(\nu_k^2 + \nu_l^2)\right]\right\}. \quad (5)$$

where, DFT is the Discrete Fourier Transform and DFT^{-1}, the inverse DFT; m, n, k, l are integers ($-N/2 < m,n,k,l \leq N/2$); d, the reconstruction distance; $A = \exp(i2\pi d/\lambda)/(i\lambda d)$; λ, the wavelength; $\nu_k = k/(N\Delta x)$, $\nu_l = l/(N\Delta y)$ are the coordinates in the spatial frequencies. Generally the digital reference wave $\boldsymbol{R}_D$ is assumed to be a normalized plane wave given by:

$$\boldsymbol{R}_D = \exp\left[i(k_x k\Delta x + k_y l\Delta y)\right]. \quad (6)$$

Let us define a more general formulation of the reconstruction in CF by replacing $\boldsymbol{R}_D$ with a complex numbers array Γ^H_{RCH} (the same can be done for SFTF) and by replacing the specimen hologram with a filtered hologram [1] containing only the virtual image frequencies [the inverse Fourier transform of the filtered spectrum defined by the area inside the window delimitated by manually drawn white lines of Fig. 2(c). (This filtering operation can be easily automated)]:

$$\Psi_{\mathrm{CF}}(m,n) = A \cdot \mathrm{DFT}^{-1}\left\{\mathrm{DFT}\left[\Gamma^H_{RCH}(k,l) I^F_H(k,l)\right] \cdot \exp\left[-i\pi\lambda d(\nu_k^2 + \nu_l^2)\right]\right\}, \quad (7)$$

with the filtered hologram written as:

$$I^F_H = \boldsymbol{R}^* \boldsymbol{O} = |\boldsymbol{R}||\boldsymbol{O}| \exp\left[-i(k_x x + k_y y)\right] \exp\left[i(\varphi + W_{\boldsymbol{O}_0} - W_{\boldsymbol{R}})\right]. \quad (8)$$

Equations 5 and Eq. 8 show that the term $W_{\boldsymbol{O}_0} - W_{\boldsymbol{R}}$, describing aberrations, is propagated into the reconstruction plane. The key point of our method is to compensate for the aberrations in the hologram plane with the introduced Γ^H_{RCH} array defined as a Reference Conjugated Hologram. This can be achieved by recording a hologram corresponding to a blank image, e.g. an experimental configuration without the presence of any specimen [Fig. 2(b)]. In reflection configuration it can be achieved by using a mirror or a flat area of the specimen holder and in transmission configuration the specimen (here the step of the USAF test target) can be moved out of the field of view. This blank hologram is filtered, (in this case manually but an automated

#69116 - $15.00 USD Received 21 March 2006; revised 3 May 2006; accepted 5 May 2006

procedure has also been defined to suppress user intervention) to retain only the virtual image [Fig. 2(d)]:

$$I_H^{R,F} = \boldsymbol{R}^* \boldsymbol{O}_0 = |\boldsymbol{R}||\boldsymbol{O}_0| \exp\left[-i(k_x x + k_y y)\right] \exp\left[i(W_{\boldsymbol{O}_0} - W_{\boldsymbol{R}})\right]. \quad (9)$$

Thus, we define Γ_{RCH}^H as the conjugated phase of Eq. 9:

$$\Gamma_{RCH}^H(m,n) = \exp\left[i \arg\left(I_H^{R,F*}\right)\right] = \exp\left[i(k_x x + k_y y)\right] \exp\left[-i(W_{\boldsymbol{O}_0} - W_{\boldsymbol{R}})\right]. \quad (10)$$

The multiplication of Γ_{RCH}^H with a filtered hologram recorded with a sample (Eq. 8) results in a suppression of the aberration terms:

$$\Gamma_{RCH}^H(m,n) \cdot I_H^F = |\boldsymbol{R}||\boldsymbol{O}| \exp\left[i\varphi(x,y)\right]. \quad (11)$$

Equation 7 is therefore a propagation of a plane wave modulated by the phase delay induced by the specimen, without aberrations terms. Figure 3 presents the reconstruction in CF. (a) shows the reconstruction performed with tilt compensation in the hologram plane (H plane) by centering the filtered spectrum of Fig. 2(c). The compensation for the aberrations is performed in the image plane by inserting a NPL defined as a 2D standard polynomial and computed with the fitting procedure detailed in Ref. [8]. We notice that the USAF steps are distorted in amplitude and phase and reveal a non-compensated image distortion. This distortion results from the propagation of phase aberrations from the hologram plane to the image plane. These phase aberrations are partially converted into image distortion during the propagation. Moreover, phase aberrations in the image plane are not totally compensated due to an insufficient polynomial order of the NPL (in this case a polynomial of order 7). On the other hand, Fig. 3(b) shows that the RCH method compensates totally for the phase aberrations in the hologram and image planes and almost completely for the image distortion. The distortion compensation is not complete because the assumption about the lack of amplitude aberration and image distortion in the hologram plane is not achieved. Indeed, the aberrations are important and therefore the object wave propagation distance from the lens ball pupil plane to the CCD plane cannot be neglected. Nevertheless a complete distortion compensation is possible by inserting, in addition to the NPL defined by the RCH method, a second NPL in the hologram plane adjusted manually to minimize the image distortion in image plane as presented in Ref. [9].

3. Self-RCH

The drawback of the RCH method is that it requires a reference hologram, and also assumes that the specimen does not introduce phase aberrations. In this section, we propose a method to circumvent those drawbacks, by using the specimen's hologram itself to generate a reference.

Let us assume that the object is smooth enough (i.e. does not contains abrupt edges such as the steps of USAF test target), we will use the hologram of a Trypanosoma Brucei recorded in a transmission setup configuration as an example [Fig. 4(a)]. Let us assume that only reduced aberrations are introduced, in particular a small defocus aberration in the hologram plane to avoid a spreading out of the virtual image frequencies. This is achieved by introducing a lens (RL in Fig. 1) that physically compensates for the curvature induced by the MO. Since the information of the details of the sample have higher frequencies than the aberrations (contained in the central frequency), two different spatial frequency filters are now computed automatically. First, the center of the two different circles defining the spatial frequencies filters [Fig. 4(b)] is defined by the computed position of the amplitude spectrum maximum. Then, the specimen filtered hologram I_H^F and the reference filtered hologram $I_H^{R,F}$ are defined respectively by the

#69116 - $15.00 USD Received 21 March 2006; revised 3 May 2006; accepted 5 May 2006

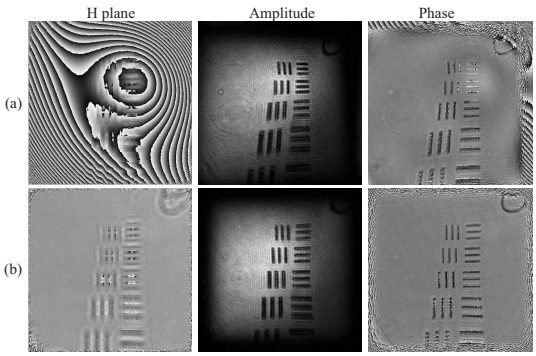

Fig. 3. The first row represents the phase in the hologram plane, the second and third one the amplitude and phase reconstructions in image plane. (a) correction of the tilt in hologram plane done by centering the filtered spectrum and the aberrations are compensated in image plane using the fitting procedure detailed in Ref. [8]; (b) aberrations compensation with Γ^{H}_{RCH}.

larger green circle (radius r_s) and the small white circle (radius r_R). The operator calibrates the circle radii only once: r_s is defined to suppress the unwanted orders (real image, zero order, parasitic interference) and to keep a maximum of specimen virtual image frequencies; r_R is defined to be as small as possible, but sufficiently large to compensate for the aberrations. In our case, this calibration gives the radii $r_s = 80$ pixels and $r_R = 10$ pixels.

It should be noticed, that the low frequencies of the specimen contained in the small radius are therefore lost but as presented in the Fig. 5, this effect can be neglected.

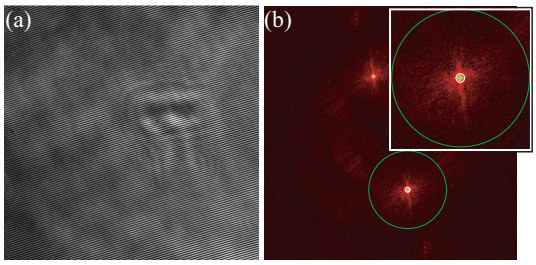

Fig. 4. (a) Hologram of Trypanosoma Brucei; (b) spectrum and detail of virtual image frequencies on the upper right; the green circle (80 pixels radius) delimits the frequency for the sample hologram and the small white one (10 pixels radius) the filtering for Self-RCH. The position of the circles' center is computed automatically by detecting the maximum of amplitude spectrum.

Figure 5(a) is a movie made of 3D plots from phase images, reconstructed from a sequence of holograms recorded at 20 frames per second. The surface around the specimen is not perfectly constant due to different noise sources such as parasitic interferences, movements of the liquid containing the specimen or defects of flatness of the specimen holder. The spatial phase noise level due to these contributions is computed using the standard deviation on the entire area around the specimen. The value obtained using this sample is about 2.7 degrees. The movement of the two unicellular animals are clearly visible, in particular the movements of the tails inside the ellipse drawn at the beginning of the movie.

#69116 - $15.00 USD
Received 21 March 2006; revised 3 May 2006; accepted 5 May 2006

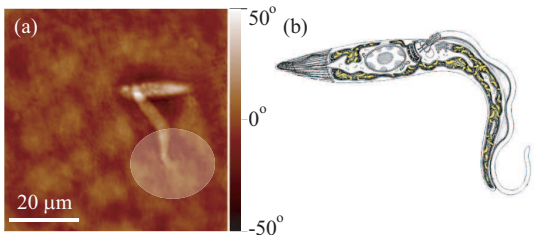

Fig. 5. (a) Phase reconstruction of Trypanosoma Brucei by Self-RCH method; (b) Schematic of the Trypanosoma Brucei.

4. Conclusion

We presented in this paper a simple calibration method called Reference Conjugated Hologram, which allows a complete aberration compensation for the phase aberrations and image distortion through the recording of a reference hologram . Furthermore, for specimens without abrupt edges, we demonstrated that the specimen hologram itself can be used to calibrate the DHM setup. The axial phase resolution is evaluated on a sequence of a unicellular animal (Trypanosoma Brucei) by measuring standard deviation of the phase around the specimen smaller than 3 degrees. The RCH and self-RCH methods demonstrates that an appropriate numerical hologram processing performed in the reconstruction procedure allows obtaining high quality phase image despite the use of low-cost optics presenting aberrations.

Acknowledgments

The authors would like to thank Julien Colomb and Prof. André Schneider (Institute of zoology, university of Fribourg, Switzerland) for providing the Trypanosoma Brucei specimen and the research grant 2153-067068.01 and 205320-103885/1 from the Swiss National Science Foundation and the research grant 6606 from the Innovation Promotion Agency (KTI/CTI).

#69116 - $15.00 USD
Received 21 March 2006; revised 3 May 2006; accepted 5 May 2006